Journal of Bone and Mineral Metabolism (2019) 37:594–606
https://doi.org/10.1007/s00774-018-0961-9

ORIGINAL ARTICLE

Effect of RAB31 silencing on osteosarcoma cell proliferation and migration through the Hedgehog signaling pathway

Qiong Yu[1] · Dong Li[2] · Dan Wang[3] · Chun-Mei Hu[1] · Yan Sun[1] · Yan Tang[1] · Guang Shi[1]

Received: 22 December 2017 / Accepted: 19 September 2018 / Published online: 23 November 2018

Abstract

Osteosarcoma (OS) is a prevalent cancer that plagues people worldwide. Identifying prognostic markers would be useful in treating human OS. In this study, we aimed to explore the functions of Ras-related protein Rab-31 (RAB31) in OS-cell proliferation, migration, and invasion as well as its roles in the Hedgehog signaling pathway for better understanding of the mechanism. To assess the detailed regulatory mechanism of RAB31 silencing on OS, both RT-qPCR and Western blot analysis were employed to evaluate the expressions of RAB31 as well as the Hedgehog signaling pathway-related genes. Besides, we also investigated the effects of silenced RAB31 both in vitro and in vivo. First, we found that in OS tissues, both mRNA and protein expressions of RAB31 and PCNA had a significant increase. Second, the Hedgehog signaling pathway was detected to play an integral role in OS progression. Finally, after transfection of RAB31-siRNA to reduce the expression of RAB31, the Hedgehog signaling pathway was suppressed, along with cell proliferation, invasion, and migration. Therefore, we conclude that RAB31 plays an important role in OS development and its silencing delays the OS progression via suppression of the Hedgehog signaling pathway.

Keywords RAB31 · Osteosarcoma · Hedgehog signaling pathway · Proliferation · Invasion

Introduction

Osteosarcoma (OS) is known to be the most common type of human primary malignant bone tumor, which has a potential propensity for both distant invasion and local invasion [1]. OS is mostly found in adolescence and children with the first incidence at the age of 15–19. It is characterized as an aggressive malignant neoplasm resulting from the primitively transformed cells originating from the mesenchyme (and thus a sarcoma) and presenting with both osteoblastic differentiation and producing malignant osteoid [2]. Moreover, a second incidence peak has been found to occur in the elderly [3], accounting for approximately 2.4% in all malignancies involving pediatric patients as well as almost 20% in all primary bone cancers [4]. Common risk factors for OS include height, birth-weight, and therapeutic radiation [5]. Currently, both chemotherapy and surgical resection are the most common therapy treatments; however, despite the improvement in therapy, the 5-year survival rate has been reported to be unsatisfactory for patients who are not responding to treatment or experiencing metastases in OS [6]. Over 40% of OS patients suffer from either recurrent or progressive diseases after experiencing the traditional first-line therapy caused by an overall poor prognosis [7]. Nevertheless, the treatment of OS has made great progress since its discovery, from traditional amputation operation onto salvage operation, neoadjuvant chemotherapy-supported limb salvage treatment, all the way to molecular-level gene therapy [8, 9]. With better understanding of the occurrence mechanism in neoplastic diseases as well as the medication dosage for the OS development, OS therapy will advance greater. To improve the OS prognosis and therapy, deeper knowledge of OS development and progression is required.

Qiong Yu and Dong Li contributed equally to this work.

✉ Guang Shi
shiguang_sg11@163.com

[1] Department of Hematology and Oncology, The Second Hospital of Jilin University, No. 218, Ziqiang Street, Changchun 130041, Jilin, People's Republic of China

[2] Department of Obstetrics and Gynecology, The Second Hospital of Jilin University, Changchun 130041, People's Republic of China

[3] Department of Breast Surgery, The Second Hospital of Jilin University, Changchun 130041, People's Republic of China

It is known that the small GTPase family Rab members are potentially essential factors in both cancer progression and development [10]. A member of the Rab5 subfamily, known as small GTPase Ras-related protein Rab-31 (RAB31), has been identified as an influencer in cancer progression and is correlated with prognosis in many types of cancer [11, 12]. One example is that production of RAB31 transcripts increased in breast-cancer cells, and high RAB31 levels were significantly correlated to the distant invasion-free survival as well as the overall survival [13]. Other than breast cancer, RAB31 has also been reported as one of the cohort (race)-dependent elements that have correlations with glioblastoma survival [14]. Apart from RAB31, Hedgehog signaling was also known to be widely involved in the development of multiple cancers and inhibition of the Hedgehog signaling in human OS led to suppression of cell proliferation and enhancement of cell apoptosis [15]. Moreover, the Hedgehog signaling was able to interfere stem cell homeostasis in adult tissues, and persistent Hedgehog pathway activity has pathological consequences in various cancers, such as the brain tumor medulloblastoma and the skin cancer basal cell carcinoma [16]. Through the scientific findings illustrated above, they demonstrated the essential role of RAB31 in cancer proliferation, progression, and apoptosis, suggesting that RAB31 may be an effective and useful candidate for the clinical therapy in most cancers [17]. Due to the fact that the role of RAB31 in OS remained unclear, in this study, we intended to investigate the effects of RAB31 silencing on both OS cell proliferation and invasion through the Hedgehog signaling pathway.

Materials and methods

Ethical statement

All aspects of this study are in strict accordance with the Declaration of Helsinki. All of the specimens were collected from the patients who have been informed and signed the consent.

Study subjects

In our study, OS tissues were collected from a total of 32 OS patients (aged from 8 to 35 years, average age of 22.4, 18 males and 14 females) with surgical treatment provided by the Second Hospital of Jilin University between September 2010 and March 2016. Osteochondroma tissues were collected from 10 osteochondroma patients treated with amputation (aged 16–47 years, average age of 28.8, 7 males and 3 females). All OS cases received neither radiotherapy nor chemotherapy prior to surgery. The cases were further classified into grades: grade I ($n=9$), grade II ($n=10$), and grade III ($n=13$) according to the pathological Tumor-Node-invasion staging system [18]. In addition, based on the new classification of OS provided by the World Health Organization (WHO), these cases were also divided into pelvis group ($n=16$), spine group ($n=11$), and limbs group ($n=5$) [19]; furthermore, in all these 32 cases, 19 of them are metastatic OS and 13 of them are non-metastatic OS. All collected specimen samples were preserved at − 80 °C before use.

Hematoxylin and eosin (HE) staining

The collected OS tissues were first fixed with 10% neutral buffered formalin for up to 16–18 h (5–7 days of decalcification for bone tissues). The fixed OS tissues along with the osteochondroma tissues were then dehydrated using a conventional gradient ethanol, cleaned with xylene, embedded with paraffin, and subsequently cut into 5-μm serial sections. After being spread out at 45 °C, sections were collected and baked for 1 h at 60 °C prior to xylene dewax. Subsequently, dewaxed sections were hydrated with water and then stained with HE (Beijing Solarbio Science & Technology Co., Ltd, Beijing, China) for observation of the pathological changes in OS and osteochondroma tissues under an optical microscope (CX31-LV320, Olympus microscope, Beijing, China). These tissues were dehydrated with gradient ethanol, cleaned with xylene, and sealed with neutral gum before observation.

Immunohistochemistry

Both collected OS tissues and osteochondroma tissues were embedded with paraffin and cut into 3–4 μm sections. Following the cut, the sections were then added along with 3% H_2O_2, conventionally dewaxed with xylene, and dehydrated with gradient ethanol at room temperature for 20 min, respectively, to inactivate the endogenous peroxidase. Subsequently, the sections were heated up to 90 °C for 5 min in an 80% power microwave to procure the antigen. After cooling down, the sections were incubated with rabbit anti-human RAB31 monoclonal antibodies (1:100) (ab103588, Abcam, Inc, MA, USA) and proliferating cell nuclear antigen (PCNA) monoclonal antibodies (1:100) (ab15497, Abcam, Inc, MA, USA) at 4 °C overnight. On the next day, the sections were cleaned to remove the primary antibodies before incubating with the biotin-labeled goat anti-rabbit immunoglobulin-gamma (IgG) secondary antibodies (1:1000) (ab6789, Abcam, Inc, MA, USA) at 37 °C for 30 min. After staining cell nuclei with a hematoxylin staining solution (C0105, Beyotime Biotechnology Co., Shanghai, China) for 30 s, the sections were visualized using diaminobenzidine (DAB) (P0202, Beyotime Biotechnology Co., Shanghai, China). After staining, the sections

were then dehydrated with a hydrochloric acid–ethanol and sealed up with a neutral gum before observation using an optical microscope (CX31-LV320, Olympus Corporation, Beijing, China). Random visual fields were selected for documentation. The cytoplasm and membrane of the cells that showed brownish-yellow indicated positive staining, anything else indicated negative staining.

To thoroughly evaluate the results of an IHC staining, all slides that were observed under the microscope were scored: Score 0: no staining was observed in invasive tumor cells. Score 1: weak, incomplete membrane staining in any proportion of invasive tumor cells, or weak, complete membrane staining in less than 10% of cells. Score 2: complete membrane staining that was non-uniform or weak but with obvious circumferential distribution in at least 10% of cells, or intense complete membrane staining in 30% or less of tumor cells. Score 3: uniform intense membrane staining of more than 30% of invasive tumor cells. This scale classification was based on the diagnostic criteria provided by the American Society of Clinical Oncology/College of American Pathologists 2007 guidelines [20].

Reverse transcription quantitative polymerase chain reaction (RT-qPCR)

Frozen tissues (about 100 mg) were ground for the total RNA extraction using the Trizol™ test kit (no. 16096020, Thermo Fisher Scientific, New York, USA). The RT-qPCR primers (Table 1) were designed using the biological software Primer Premier 5 and Oligo 6 and they were synthesized by Takara (Takara Bio Inc., Shiga, Japan), with glyceraldehyde-3-phosphate dehydrogenase (GAPDH) serving as the internal reference. RNA concentration and purity were evaluated using an ultraviolet–visible spectrometer to measure the optical density (OD) value at both 260 and 280 nm, respectively. The RNA samples with high purity were used for cDNA synthesis and the reaction system consisted of 5 μL Mix reagents (4368702, Tideradar Beijing technology CO., Ltd., Beijing, China), 5 μL of total RNA, and 10 μL RNase-free H_2O. The reverse transcription was conducted in a qPCR machine with the following conditions: 37 °C for 15 min, 85 °C for 5 s for transcriptase inactivation, and finally the reaction ended at 4 °C. The obtained cDNA was then stored at − 20 °C before use. The RT-qPCR was performed in an ABI 7500 real-time Thermocycler (Applied Biosystems, Foster City, Calif, USA). The conditions for the RT-qPCR were: predenaturation at 95 °C for 10 min, denaturation at 95 °C for 10 s, anneal at 60 °C for 20 s, and extension at 72 °C for 34 s with a total of 40 cycles. SYBR Green fluorescent dye (Item No. RR091A, TAKARA Bio Inc, Shiga, Japan) was used to detect the expression of RAB31, glioma-associated oncogene homolog 1 (Gli1), patched1 (PTCH1), sonic Hedgehog (shh), smoothened (smo), PCNA, bax, and bcl-2 following the 48 h of transfection (the test methods were also fit for cell experiment).

Table 1 RT-qPCR primer sequences

Gene	Primer sequences
RAB31	Forward primers: CTCGAATTCAATGATGGCGATACGGGAGCTC
	Reverse primers: TCGGTCGACTCAACAGCACCGGCGGCT
Gli1	Forward primers: CCAACCTCTGTCTACTCAC
	Reverse primers: CCTGTTCTGGCTTGACTT
PTCH1	Forward primers: GGCAGCCGCGATAAG
	Reverse primers: TTAATGATGCCATCTGCATCCA
PCNA	Forward primers: CGGTTAGAAGGGGTTA
	Reverse primers: GACGGTCTCGGTGTGT
bax	Forward primers: CAGCTCTGAGCAGATCATGAAGACA
	Reverse primers: GCCCATCTTCTTCCAGATGGTGAGC
bcl-2	Forward primers: CGCCCTGTGGATGACTGAGTA
	Reverse primers: GGGCCGTACAGTTCCACAAAG
shh	Forward primers: TCCAGAAACTCCGAGCGATTTAAG
	Reverse primers: CACTCCTGGCCACTGGTTCA
smo	Forward primers: GTTCTCCTATATCCTCCTTCTC
	Reverse primers: CTTCCTGCTGTCTGATTCTT
GAPDH	Forward primers: CGAGATCCCTCCAAAATCAA
	Reverse primers: AGGTCAGGTCCACCACTGAC

RT-qPCR reverse transcription quantitative polymerase chain reaction, *RAB31* Ras-related protein in brain 31

Western blot analysis

Frozen OS tissues and osteochondroma tissues were also ground in liquid nitrogen for protein extraction using protein lysis buffer (C0481, Sigma, St. Louis, MO, USA) and the lysate (supernatant) was collected via centrifugation at 25,764×*g* for 20 min at 4 °C. The collected lysate was subjected to protein concentration determination using the bicinchoninic acid (BCA) protein assay. Equal amount of protein samples was denatured by boiling at 100 °C for 5 min with loading buffer and then loaded on the 10% sodium dodecyl sulfate separation gel after cooling down on ice. Subsequently, the separated protein was then transferred to the nitrocellulose membranes, which were fixed using 5% skim milk powder at 4 °C overnight. On the next day, the membranes were incubated with the rabbit anti-human RAB31, Gli1, Gli2, GLi3, PTCH1, shh, smo, PCNA, bax, and bcl-2 primary antibodies ((ab103588, ab49314, ab26056, ab6050, ab53715, ab50515, ab32575, ab92552, ab32503, ab32124, Abcam, Inc, MA, USA) (1:1000) and rabbit anti-human GAPDH (ab8226, Abcam, Inc, MA, USA) (1:2000) was used as an internal reference. After 1-h incubation at room temperature, the membranes were washed with PBS for three times (5 min each time) prior to another 1-h incubation with the secondary antibodies goat anti-rabbit IgG (1:1000) (ab6785, Abcam, Inc, MA, USA) at room temperature. Membranes were subsequently washed three times (5 min each time) with PBS solution and then immersed in an electrochemiluminescence (ECL) (Pierce, Waltham, MA, USA). The ratio between the gray-scale values of the target band and internal reference (GAPDH) band was taken as the relative expression of the proteins.

RAB31 adenovirus expression vector construction

To construct the adenovirus vectors for targeting RAB31 (siRNA-RAB31), overexpressing RAB31 (Ad-CMV-RAB31-eGFP), as well as an empty adenovirus vector (Ad-CMV-eGFP) as a negative control, the recombinant plasmid pLenR-GPH vector (Engreen Biosystem Co., Ltd, Beijing, China) was used. According to the RAB31 mRNA sequences (1, 5′-GGAUCACUUUGACCACCACAAC-3′, 2, 5′-GGAUGCUAAGGAAUACGCU-3′, and 3, 5′-GCA GGAUUCAUUUUAUACC-3′) found in NCBI nucleotide database, the specific siRNA sequence targeting RAB31 was designed and its correlated double-stranded DNA oligo was synthesized, which were later ligated into pLenR-GPH vector using enzyme digestion method.

Cell transfection

Human OS cell line MG-63 (Beijing union medical center, Beijing, China) as well as the human osteochondroma cells SW1353 (Beijing Kyushu Tianrui Technology Co., Ltd, Beijing, China) was cultured in a RPMI1640 cell culture medium (22400089, Gibco, Gaitherburg, MD, USA) with a 10% fetal bovine serum (FBS). The cells were then subcultured in a 6-well plate with a cell density of 1×10^5 cells per well under optimal growth conditions (37 °C, 5% CO_2, saturated humidity). During the cell growth, the cell culture medium was replaced every 2 or 3 days according to cell growth condition, and the cell passage was conducted when the cell confluence reached between 80 and 90%. For cell passage, after removal of the cell culture medium, cells were washed twice with the PBS solution and detached using 0.25% trypsin for 2–5 min. Subsequently, cells were resuspended in 5 mL RPMI1640 (22400089, Gibco, Gaitherburg, MD, USA) culture medium that contained 10% FBS for cell distribution.

When the cells were in the logarithmic growth phase, they were used for overnight inoculation for transfection. In total 1×10^5 cells per well were inoculated in a 6-well plate on the day before transfection and it would reach 70–80% confluency on the next day. According to the treatments, cells were grouped into six groups: (1) the control group (human osteochondroma cells, without transfection), (2) blank group (human OS cells, without transfection), (3) NC group (human OS cells, transfected with Ad-CMV-eGFP), si-RAB31 group (human OS cells, transfected with si-RAB31), (4) OE-RAB31 group (human OS cells, transfected with Ad-CMV-RAB31-eGFP), (5) Hedgehog pathway inhibitor—Cyclopamine + eGFP group (Cyclopamine, 10 μM, Toronto Research Chemicals, Toronto, Canada), and (6) Cyclopamine + OE-RAB31 group (co-transfected with OE-RAB31 and Cyclopamine). The cell transfection was conducted in accordance with the instructions provided by the LiPofectamine® 2000 transfection reagent (11668-019, Invitrogen, New York, California, USA). In total, 500 μL of the serum-free Opti-MEM medium (Gibco, Gaitherburg, MD, USA) was used per transfection: half of them was used to dilute the vectors (100 pmol each), namely Ad-CMV-eGFP, siRNA-RAB31, and Ad-CMV-RAB31-eGFP to a final concentration of 50 nM, followed by thorough mixing and incubation at room temperature for 5 min; another half was used to mix with 5 μL LiPofectamine 2000. At the end, the aforementioned two diluted medium complexes were then mixed together, incubated for 5 min at room temperature before adding into the wells. After transfection, cells were continued to be inoculated at 37 °C with 5% CO_2 for 6–8 h before changing the cell medium to a complete medium. Following a 24-h incubation, the protein in the cells was detected under a fluorescence microscopy (M30C, Shanghai Wanheng Precision Instrument Co., Ltd, Shanghai, China). Two expression areas were both preserved in the form of pictures to calculate the average value afterwards.

Transfection rates as well as the transfected cells/total number of cells were calculated.

3-(4, 5-dimethylthiazol-2-yl)-2, 5-diphenyltetrazolium bromide (MTT) assay

After 24 h of transfection, the cells that were in logarithmic growth phase were resuspended in a RPMI 1640 culture medium with 10% FBS to obtain a cell density of 2.5×10^5 cells/mL, which were then inoculated in a 96-well culture plate. With 8 wells/group and 100 μL of cell suspension/well, the cells were further incubated (5% CO_2, 37 °C) for 24, 48, and 72 h and their OD value at those three time points was also measured. The OD measurement was conducted according to the following steps: MTT solution (5 mg/mL) (Sigma, SF, USA) was added to the transfected cells for another 4 h incubation; after discarding the supernatant, 150 μL of dimethyl sulfoxide (DMSO) was added to each well and incubated for 10 min to fully dissolve it; subsequently the OD value was measured at 490 nm with an automatic microplate reader (Bio-Rad, Hercules, Cal, USA). Three parallel wells were used to represent one group to obtain the mean value, and the experiment was repeated for 3 times. The cell growth curve was graphed using the MTT processing time as the *x*-axis and OD value as the *y*-axis.

Clonogenic assay

Cell suspension was generated by detaching the cells that were in logarithmic growth phase with 0.25% trypsin and then seeded in a 6-well plate for incubation with complete medium for up to 12–14 days. Starting from the day 4 of incubation, the culture medium was changed every 2 days until significant cell cloning was observed, and then the cell culture was collected for methylene blue staining after being washed with PBS. Stained cells were both photographed and counted using a BIO-RAD imaging system (Bio-Rad, Hercules, Cal, USA). This experiment was also repeated three times.

Transwell assay

A Matrigel (no. 356234, BD, San Jose, CA, USA) solution was used to suspend the cells and the cell–Matrigel suspension was incubated overnight at 4 °C. On the next day, cell–Matrigel suspension was diluted using a serum-free medium into a ratio of 1:3, and then transferred 50 μL suspension/well into the upper chamber of a Transwell chamber, followed by equilibrium in a culture incubator for 30 min. Then, 1×10^5 cell/mL cell suspension was inoculated in the upper chamber. Meanwhile, the medium containing 10% FBS was added into the lower chamber. After 24 h-inoculation, the number of cells that passed through the Matrigel was measured, which was used as an index to evaluate the invasion and metastasis capacity of cells. The experiment was repeated a total of three times.

Scratch test

For conducting the scratch test, approximately 5×10^5 cells were evenly seeded in the 6-well plate and five horizontal lines were marked on the back of the 6-well plate for labelling the scratch location for the next day. Wounds were scratched perpendicularl to the marked line on the bottom of each well with a sterile pipette tip, followed by washing three times with PBS to remove scratched cells. After adding the serum-free medium, the cells were placed back to a 37 °C incubator with 5% CO_2 for incubation and samples were collected and photographed at 0 and 24 h.

Cell cycle and cell apoptosis observation using flow cytometry

The transfected cells were collected after 48-h transfection and they were washed with PBS and detached with 0.25% trypsin until cells had morphed into a round shape. To terminate the detachment, the 0.25% trypsin was discarded and the serum culture medium was used to resuspend the cells. The cell suspension was centrifuged at 179×*g* for 5 min to remove the supernatant and then the cells were washed twice with PBS and incubated with pre-cooled 70% ethanol for 30 min. After centrifugation, cells were collected and washed with PBS, followed by 30-min staining using a 1% propidium iodide (PI) containing RNA enzyme. Once the staining procedure was finished, cells were washed twice with PBS to remove the PI and the final volume was adjusted to 1 mL using PBS. The IP-stained cell suspension was subjected to flow cytometry (FACS Calibur, Beckman Coulter, Fullerton, CA, USA) to analyze the cell cycle by recording the red fluorescence at an excitation wavelength of 488 nm. Each group had three samples and the experiment was repeated 3 times.

The cells that were transfected after 48 h were also used for Annexin-V-FITC staining to observe cell apoptosis. Transfected cells were detached using ethylenediaminetetraacetic acid (EDTA)-free trypsin, and detached cells were centrifuged to remove the supernatant and then washed three times using cold PBS. Meanwhile, in strict accordance with the instructions provided by the Annexin-V-FITC apoptosis detection reagent kit (C1065, Beyotime Biotechnology, Shanghai, China), Annexin-V-FITC/PI dye solution was prepared using the Annexin-V-FITC, PI, and HEPES buffers at a ratio of 1:2:50. When both cells and dye solution were ready, 100 μL dye solution was used to resuspend the cells to reach a density of 1×10^5 cells/mL. After incubating the cell suspension at room temperature for 15 min, 1 ml HEPES

buffer was added to the cell suspension. Stained cells were subjected to FITC and PI fluorescence detection to evaluate cell apoptosis under an excitation wavelength of 488 nm and the detection wavelength was 525 nm for FITC fluorescence and 620 nm for PI fluorescence. Each group had three samples and the experiment was repeated 3 times.

Statistical analysis

Data were processed and analysed using a statistic software SPSS 21.0 (IBM Corp. Armonk, NY, USA). The measurement data were expressed using the mean ± standard deviation. Student's *t* test was applied for comparison between two groups and analysis of variance (ANOVA) for comparison among groups. When $p < 0.05$, then the comparison is considered to be significantly different.

Results

RAB31 may be involved in the progression of OS

HE staining, immunohistochemistry, RT-qPCR, and western blot analysis were performed to examine the involvement of RAB31 in OS development. The result of HE staining on osteochondroma tissue (left panel of Fig. 1a) shows fibrous chondroma and cartilage matrix, and chondrocytes are in the cavity with mixed cartilage tissue and cancellous bone. However, OS tissues (right panel of Fig. 1a) showed accumulation of tumor cells with clear nucleus, in which the nuclear chromatin showed an increasing trend, leading to both increased and enlarged nuclear particles as well as darker staining, with a visible mitotic as well as a visible tumor-like bone formation and labyrinthoid bone-like matrix between the heterogeneous spindle cells. OS cells also showed an infiltration growth and invasion regarding peripheral bone tissues. The results of the immunohistochemistry (Fig. 1b) indicate that RAB31 was highly expressed in cytoplasm while PCNA was highly expressed in the nucleus. In addition, the protein expression levels of RAB31 and PCNA were both significantly higher in OS tissues than in osteochondroma tissue ($p < 0.05$) (Fig. 1c). Furthermore, both RT-qPCR and Western blot analysis results (Fig. 1d) provided evidence indicating that the transcript levels of the RAB31 and PCNA were notably elevated in OS tissues, in comparison with osteochondroma tissues (all $p < 0.05$).

RAB31 accelerates the development of OS

To determine the correlation between RAB31 expression and clinical features, bone tissues collected from different patients were analyzed. No significant correlation was found between the expression of RAB31 in bone tissues with the age, gender, and the tumor location of OS patients ($p > 0.05$). However, patients who had a larger tumor diameter, severe clinical stage, higher degree of differentiation and metastasis showed higher RAB31 expression ($p < 0.05$), indicating that expression of RAB31 was directly correlated to the occurrence and development of OS, as well as promoting the malignant progression of the tumor (Table 2).

Hedgehog signaling pathway may be involved in OS development

Hedgehog signaling pathway has been reported to be a pathway that played an important role in OS development [15, 21]. To verify the role of Hedgehog signaling pathway in OS, we conducted western blot analysis and the results (Fig. 2) showed that, when compared with the osteochondroma tissues, protein levels of Gli1, Gli2, PTCH1, shh, smo, and bcl-2 were all significantly increased in OS tissues (all $p < 0.05$), while the bax protein level was significantly decreased ($p < 0.05$). No change in the Gli3 expression was found in any of the groups. Taking these results into consideration, we came to the conclusion that the Hedgehog signaling may be involved during the development of OS.

Adenovirus vectors are successfully transfected into osteochondroma cells and OS cells

To confirm whether the transfection was successful, fluorescence from all the transfected cells was observed under fluorescence microscopy but no green fluorescence signal was detected in the control, blank, and the Cylopamine group. While intensive green fluorescence signal (protein expression rate reaching over 80%) was detected in the NC group, the si-RAB31 group, the OE-RAB31 group, and the Cylopamine + OE-RAB31 group, indicating that the adenovirus vectors were successfully transfected into osteochondroma cells and OS cells and they were also expressed in cells effectively (Fig. 3).

RAB31 positively regulates Hedgehog signaling pathway

Apart from investing the role of Hedgehog signaling pathway in OS, western blot assay was also employed to study the regulatory mechanism of RAB31 on Hedgehog signaling pathway. In comparison with the control group, RAB31-siRNA transfected group showed significant downregulation of RAB31 protein expression (Fig. 4a, b). While in the other groups, the protein expressions of RAB31, Gli1, Gli2, PTCH1, shh, smo, PCNA, and bcl-2 were significantly higher ($p < 0.05$) and the expression of bax was significantly lower than that in the control group ($p < 0.05$). The protein expressions of RAB31, Gli1, Gli2, PTCH1, shh,

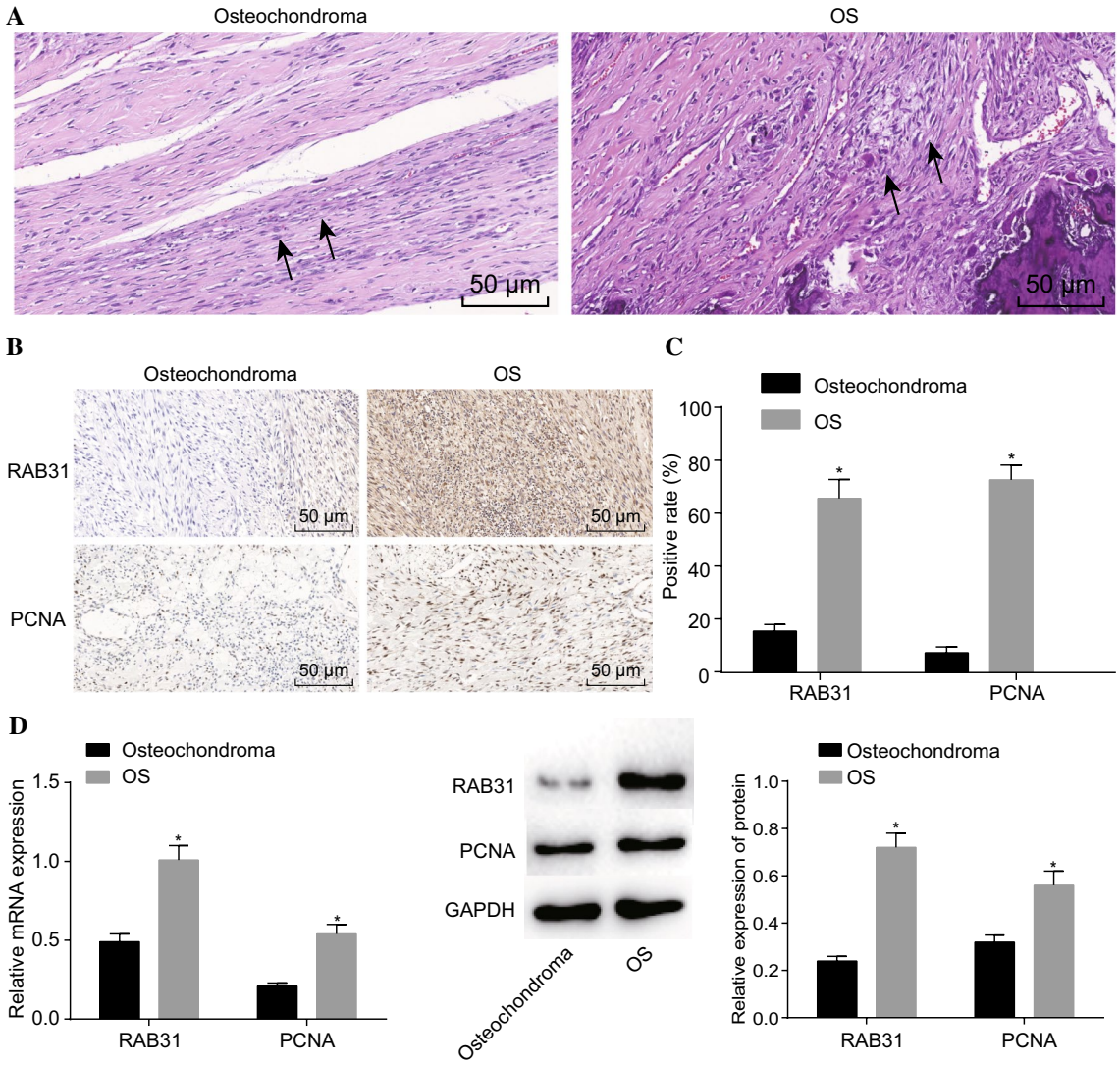

Fig. 1 RAB31 plays a part in the progression of OS. **a** HE staining (100×) of osteochondroma tissues and OS tissues, arrow refers to the cartilage tissue; **b** immunohistochemistry results presented that RAB31 was mainly expressed in the cytoplasm and PCNA was mainly expressed in the nucleus, and OS tissues had higher expression of RAB31 and PCNA (400×); **c** Western blot analysis results proved that PCNA protein expression was significantly higher in the OS tissues when compared with the osteochondroma tissues; **d** RT-qPCR and western blot analysis results showed that mRNA and protein expression of RAB31 and PCNA was higher in OS tissues; *$p < 0.05$ compared with osteochondroma tissues; *HE* hematoxylin and eosin; OS, osteosarcoma, *RAB31* Ras-related protein Rab-31, *PCNA* proliferating cell nuclear antigen

smo, PCNA, bcl-2, and bax all showed no significant differences among the blank group and the NC group ($p > 0.05$). In comparison with the NC group, the protein expression of Gli1, Gli2, PTCH1, shh, smo, PCNA, and bcl-2 were all significantly decreased, while the expression of bax showed a significant increase in both the si-RAB31 and Cylopamine groups (all $p < 0.05$); the protein expression of Gli1, Gli2, PTCH1, shh, smo, PCNA, and bcl-2 had all significantly increased, in contrary, the expression of bax was showing significant decrease in the OE-RAB31 group (all $p < 0.05$). No remarkable change in Gli3 expression was observed in any group ($p > 0.05$). The protein expression of Gli1, Gli2, PTCH1, shh, smo, PCNA, bcl-2, and bax in the Cylopamine + OE-RAB31 group was higher than that in the Cylopamine group, but lower than that in the OE-RAB31 group ($p < 0.05$). Based on the aforementioned findings, it seems that Hedgehog signaling pathway is negatively regulated by RAB31.

RAB31 silencing inhibits OS cell proliferation while promoting apoptosis

To confirm the effects of RAB31 on OS progression, we conducted an MTT assay (Fig. 5a), clonogenic assay (Fig. 5b,

Table 2 Correlation of expression of RAB31 and the clinicopathological features of OS patients

Clinicopathological features	Numbers	RAB31 expression		*p*
		+	–	
Age				
≥ 15	25	10	15	0.6691
< 15	7	4	3	
Gender				
Male	18	9	9	0.4896
Female	14	5	9	
Tumor site				
Spine	11	3	8	0.3234
Pelvis	16	9	7	
Limbs	5	2	3	
Tumor diameter				
≥ 5 cm	18	14	4	< 0.0001
< 5 cm	14	0	14	
Tumor metastasis				
Metastatic	19	14	5	< 0.0001
Non-metastatic	13	0	13	
Clinical stages				
Stage I–II	19	1	18	< 0.0001
Stage III	13	13	0	
Differentiation degree				
Moderate and low	14	14	0	< 0.0001
High	18	0	18	

RAB31 Ras-related protein in brain 31, *OS* osteosarcoma

c), and a flow cytometry (Fig. 5d–g). In comparison with the control group, the cell proliferation, cloning ability, and cells arrested at S phase of other groups all significantly increase accompanied with reduced apoptosis rate ($p < 0.05$). No significant difference was detected in the cell growth between the blank group and NC group at any time point (24 h, 48 h, 72 h of transfection) ($p > 0.05$). When comparing with the NC group, both the cell growth and cloning abilities found in the si-RAB31 and Cylopamine groups were all significantly reduced at each time point with decreased number of cells arrested at the S phase and a higher apoptosis rate ($p < 0.05$), while the OE-RAB31 group showed the opposite results ($p < 0.05$). The above changes in the trend at different time intervals in the Cylopamine + OE-RAB31 group were found between the Cylopamine group and the OE-RAB31 group ($p < 0.05$). To summarize, RAB31 negatively influences the OS cell proliferation and the inhibition of RAB31 expression increases OS cell apoptosis rate.

RAB31 silencing suppresses OS cell migration and invasion

Beside exploring the effect of RAB31 in cell proliferation and apoptosis, we also investigate how RAB31 affects the OS cell migration and invasion using Transwell assay and scratch test. On one hand, the results from Transwell assay (Fig. 6a, b) showed that the cell migration ability of the control group was significantly weaker than the other 5 groups ($p < 0.05$). The blank and NC group had no significant difference in the number of migrated cells detected under a microscope ($p > 0.05$). When comparing the si-RAB31 and Cylopamine group with the NC group, si-RAB31 and Cylopamine groups had lower amount of migrated cells ($p < 0.05$) while the OE-RAB31 group had significantly more migrated cells ($p < 0.05$). The number of migrating cells in the Cylopamine + OE-RAB31 group was more in the si-RAB31 but less in the OE-RAB31 groups

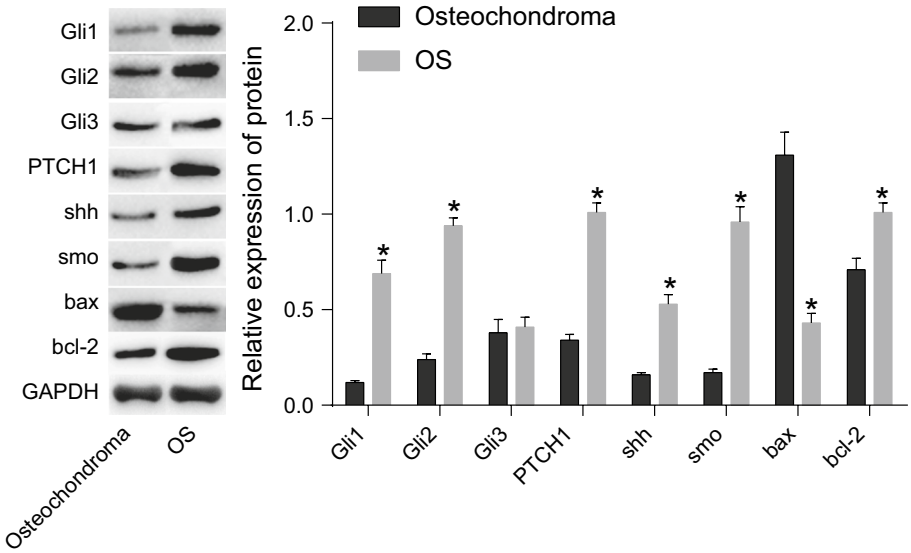

Fig. 2 Hedgehog signaling pathway affects the development of OS. **a** Protein expression of different members of the Hedgehog signaling pathway in western blot analysist; **b** quantified relative protein expression level of different members of the Hedgehog signaling pathway; *$p < 0.05$ compared with osteochondroma tissues; *HE* hematoxylin and eosin, *OS* osteosarcoma

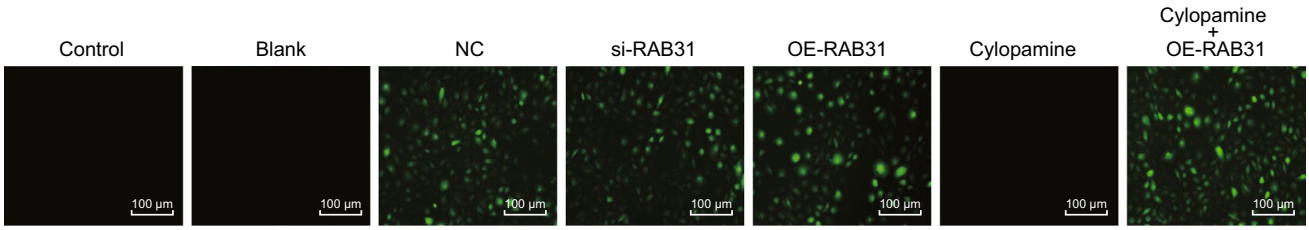

Fig. 3 Successful transfection of adenovirus vectors into osteochondroma cells and OS cells (×100). **a** Phase-contrast images of seven transfected groups; **b** adenovirus vectors were successfully transfected into osteochondroma cells and OS cells; *OS* osteosarcoma, *RAB31* silencing RAB31, *OE-RAB31* over-expression RAB31, *RAB31* Ras-related protein Rab-31

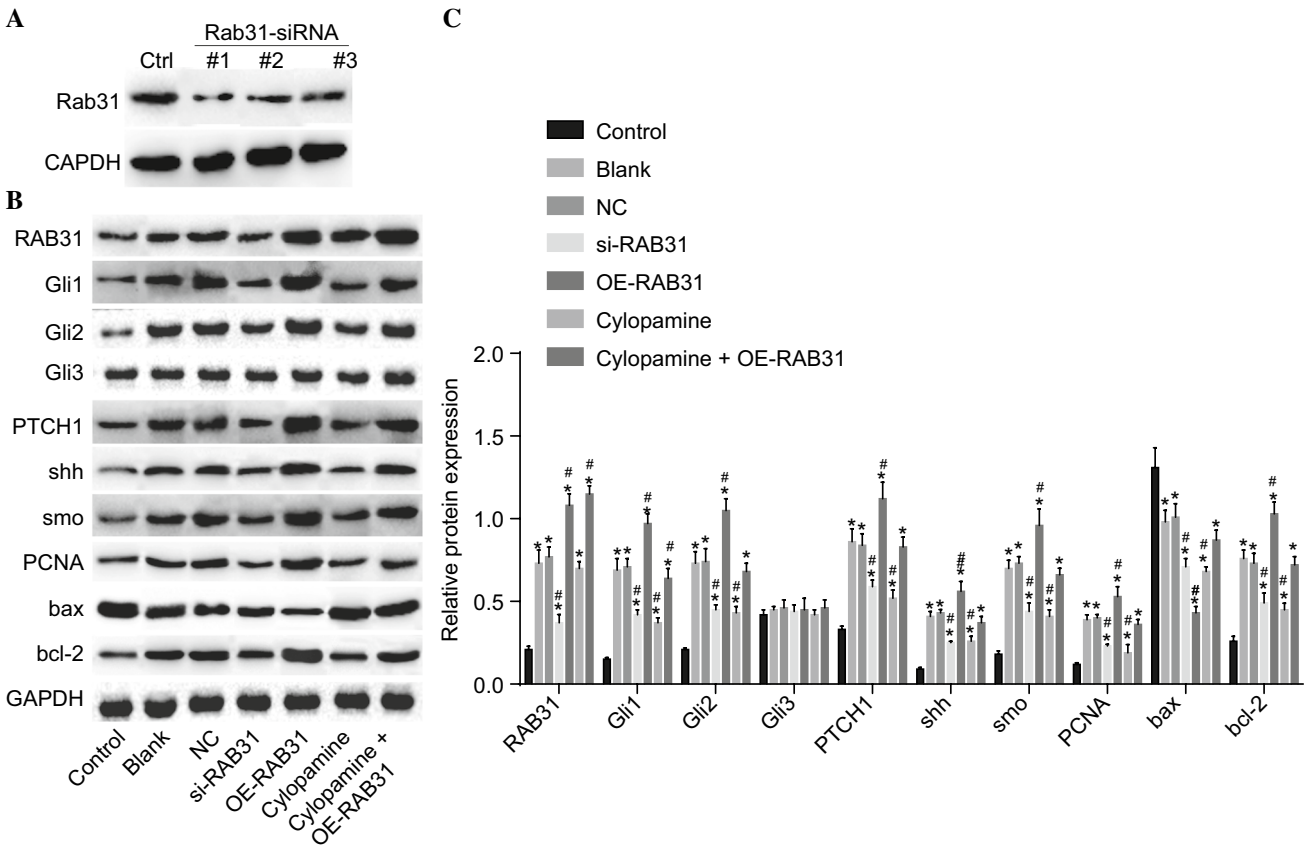

Fig. 4 Silencing of RAB31 inhibits the Hedgehog signaling pathway. **a** Protein expression of RAB31 and 4 different groups (control, 1–3 group); **b**, **c** western blot analysis was conducted for analyzing the expression of RAB31, Gli1, Gli2, Gli3, PTCH1, shh, smo, PCNA, bax, and bcl–2; $^{*}p < 0.05$ compared with the control group; $^{\#}p < 0.05$ compared with the blank group; *NC* negative control, *OS* osteosarcoma, *si-RAB31* silencing RAB31, *OE-RAB31* over-expression RAB31, *RAB31* Ras-related protein Rab-31

($p < 0.05$). On the other hand, the scratch test (Fig. 6c, d) results reveal that the migration ability in the other groups had significantly improved compared to the control group ($p < 0.05$), while the blank and NC groups had no significant differences in cell migration ability in terms of cell number ($p > 0.05$). In comparison with the NC group, the migration ability was significantly suppressed in both the si-RAB31 and Cylopamine groups ($p < 0.05$) while the OE-RAB31 group showed significantly higher cell migration ability ($p < 0.05$). These evidences indicate that OS progression was delayed by RAB31 silencing.

Discussion

Unsatisfactory survival rates among the OS patients drives the mechanistic research in OS to develop respectable approaches such as therapy involving molecularly targeted

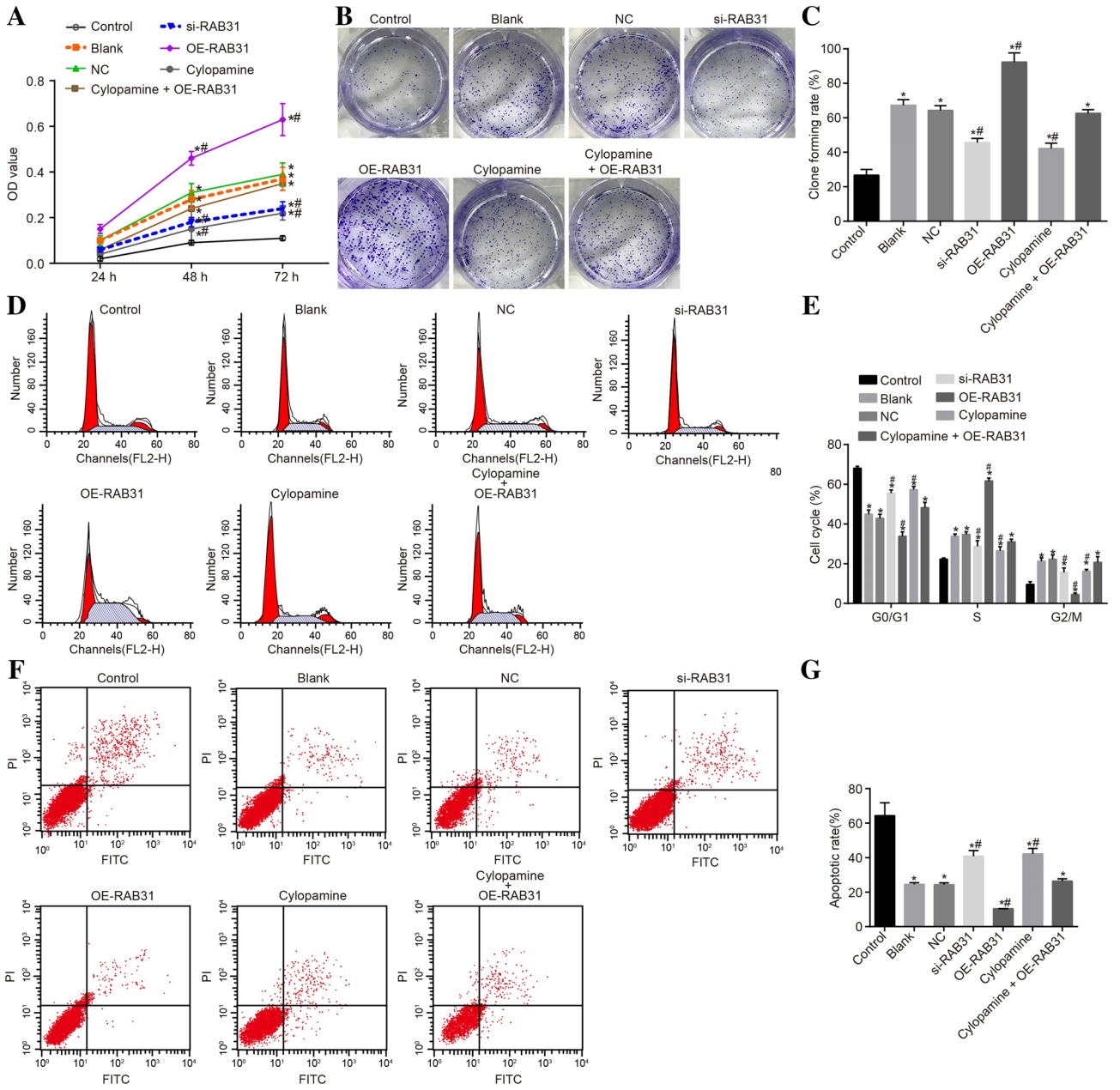

Fig. 5 RAB31 inhibition suppresses proliferation while improving OS cell apoptosis (200×). **a** OD value of different transfected groups from 3 time points: 24 h, 48 h, and 72 h, respectively; **b** cells during logarithmic growth phase were seeded on a 6-well plate and cultured for 12–14 days until obvious colony formation was observed. Afterwards, cells were photographed and counted. The experiment was repeated three times; **c** clonogenic assay proved that RAB31 silencing decreased colony formation rate; **d**, **e** scratch test manifested that RAB31 depletion reduced cells arrested at S phase; **f**, **g** flow cytometry results verified that apoptosis was induced by RAB31 depletion; $^{*}p < 0.05$ compared with the control group; $^{\#}p < 0.05$ compared with the blank group; *NC* negative control, *OS* osteosarcoma, *si-RAB31* silencing RAB31, *OE-RAB31* over-expression RAB31, *RAB31* Ras-related protein Rab-31

drugs or gene therapy, which could become a breakthrough in future OS treatment [22, 23]. In this study, we aimed to demonstrate the effect of RAB31 and its silencing on OS cell proliferation, and migration as well as the effect of RAB31 on the Hedgehog signaling pathway.

The expression of RAB31, Gli1, PTCH1, shh, smo, PCNA, and bcl-2 were all increased except the expression of bax, which was reduced in OS tissues when compared with the osteochondroma tissues. Higher RAB22A expression was demonstrated in human OS cells and tissues [24]

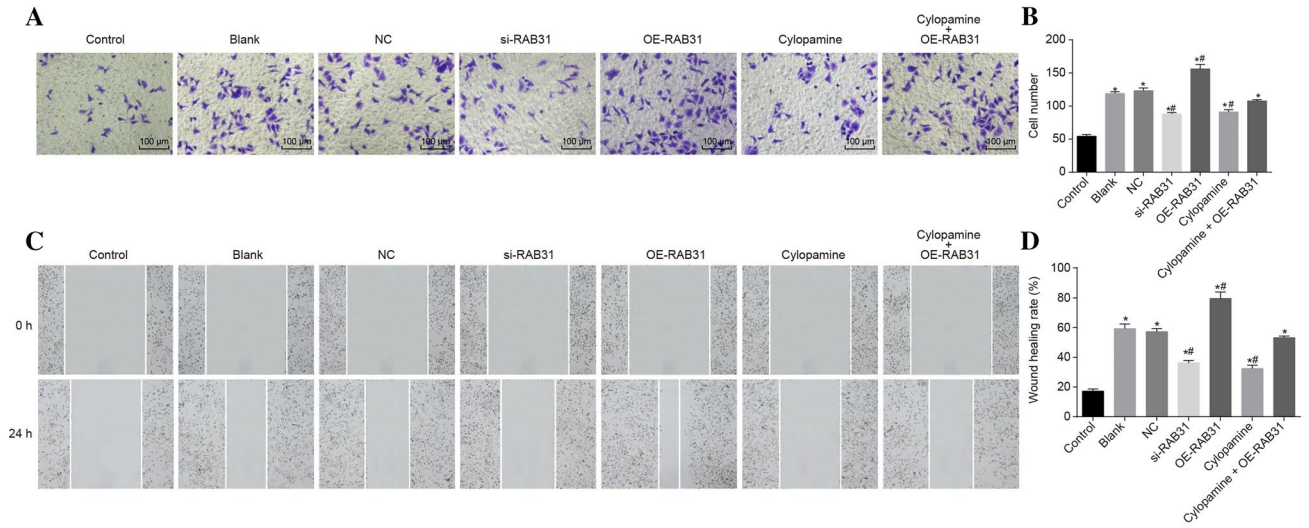

Fig. 6 RAB31 inhibition exerts negative function on OS cell migration and invasion. **a**, **b** transwell assay proved that OS cell invasion was inhibited by RAB31 depletion; **c**, **d** scratch test verified that OS cell migration was inhibited by RAB31 depletion; $^{*}p<0.05$ compared with the control group; $^{\#}p<0.05$ compared with the blank group (×200); *NC* negative control, *OS* osteosarcoma, *si-RAB31* silencing RAB31, *OE-RAB31* over-expression RAB31, *RAB31* Ras-related protein Rab-31

and another study showed elevated expression of RAB31 in breast cancer with RAB31 having some effects on breast cancer, cervical cancer, and glioblastoma progression [10]. It has been reported that Gli1 was highly expressed in multiple canine OS cell lines [25], which is consistent with our results. A study that was focused on the Hedgehog signaling pathway and the pathogenesis of osteosarcoma found that OS cell lines had over-expression of shh, PTCH1, smo, and Gli [26]. In line with our study, high levels of PCNA immunoreactivity have been showed in the nucleus and/or cytoplasm of the OS cells [27]. Elevated bcl-2 activity was also found in OS tissues when compared with the normal bone tissue [28]. In addition, high expression of bax was also observed in OS cells, while treated with different concentrations of Bufalin, the expression of bax in OS cells was reduced [29].

Besides, our study reported that RAB31 silencing in OS cell suppressed the Hedgehog signaling pathway. In bacteria, once the single domain nucleotide-dependent molecular switches, the Ras superfamily of small GTPases acts as highly tuned regulators of complex signal transduction pathways and was able to control complex functions including motility, cell polarity, predation, antibiotic resistance, and development [30]. In OS, the Hedgehog signaling pathway is aberrantly activated, and suppression of the Hedgehog receptor could induce apoptosis and growth arrest of OS cells both in vivo and in vitro [31]. Furthermore, suppressing the Hedgehog signaling can also control OS cell proliferation [32]. Combining standard FDA-approved anticancer agents and Hedgehog signaling pathway inhibitors can be a potentially beneficial therapeutic method for treating OS [33]. Gli1, PTCH1, shh, and smo are all components involved with Hedgehog signaling pathway [34–36]. Therefore, we concluded that RAB31 silencing suppressed the Hedgehog signaling pathway in OS.

We also found that cells transfected with si-RAB31 had reduced cell proliferation and migration ability and elevated apoptosis rate through inhibition of the Hedgehog signaling pathway. It has been reported that RAB31 can promote cell proliferation as well as migration/invasion in glioblastoma and cervical cancer [17]. A higher expression of RAB31 in breast cancer cells resulted in a switch from an invasive phenotype towards a proliferative phenotype with indications such as elevated level of cell proliferation, inhibited adhesion, and invasion in vitro, as well as a decreased capacity of lung metastases formation [12]. In addition, silencing of RAB31 was shown to induce cell apoptosis and inhibit the MHCC97 cells' growth capacity [37]. Meanwhile, the Hedgehog pathway can also regulate the cell proliferation and organ/tissue differentiation during development, and hence suppression of the Hedgehog signaling pathway could be used as particular targeted therapy for OS [38]. Furthermore, RAB23 was considered as an essential negative regulator of the mouse Sonic Hedgehog signaling pathway [39].

In conclusion, our study identified the important role of RAB31 in OS and RAB31 silencing could be beneficial for treating OS as it inhibits both the OS cell proliferation and invasion via the Hedgehog signaling pathway. Although our findings have strong implications for therapeutic development in OS treatment, the mechanism mediating the interaction between both the RAB31 and Hedgehog signaling pathway in OS still requires further elucidation.

Acknowledgements We thank the reviewers for critical comments.

Compliance with ethical standards

Conflicts of interest The authors declares that they have conflict of interest.

Ethical approval All aspects of the study are in strict accordance with the Declaration of Helsinki. All of the above specimens were collected with informed consent of patients and all the patients signed informed consent.

References

1. Liu T, Zhou W, Zhang F, Shi G, Teng H, Xiao J, Wang Y (2014) Knockdown of IRX2 inhibits osteosarcoma cell proliferation and invasion by the AKT/MMP9 signaling pathway. Mol Med Rep 10:169–174
2. Luetke A, Meyers PA, Lewis I, Juergens H (2014) Osteosarcoma treatment—where do we stand? A state of the art review. Cancer Treat Rev 40:523–532
3. Savage SA, Mirabello L (2011) Using epidemiology and genomics to understand osteosarcoma etiology. Sarcoma 2011:548151
4. Huang J, Ni J, Liu K, Yu Y, Xie M, Kang R, Vernon P, Cao L, Tang D (2012) HMGB1 promotes drug resistance in osteosarcoma. Cancer Res 72:230–238
5. Mirabello L, Pfeiffer R, Murphy G, Daw NC, Patino-Garcia A, Troisi RJ, Hoover RN, Douglass C, Schuz J, Craft AW, Savage SA (2011) Height at diagnosis and birth-weight as risk factors for osteosarcoma. Cancer Causes Control 22:899–908
6. Wang Y, Li L, Shao N, Hu Z, Chen H, Xu L, Wang C, Cheng Y, Xiao J (2015) Triazine-modified dendrimer for efficient TRAIL gene therapy in osteosarcoma. Acta Biomater 17:115–124
7. Bienemann K, Staege MS, Howe SJ, Sena-Esteves M, Hanenberg H, Kramm CM (2013) Targeted expression of human folylpolyglutamate synthase for selective enhancement of methotrexate chemotherapy in osteosarcoma cells. Cancer Gene Ther 20:514–520
8. Xu M, Xu SF, Yu XC (2014) Clinical analysis of osteosarcoma patients treated with high-dose methotrexate-free neoadjuvant chemotherapy. Curr Oncol 21:e678–684
9. Oertel S, Blattmann C, Rieken S, Jensen A, Combs SE, Huber PE, Bischof M, Kulozik A, Debus J, Schulz-Ertner D (2010) Radiotherapy in the treatment of primary osteosarcoma—a single center experience. Tumori J 96:582–588
10. Chua CE, Tang BL (2015) The role of the small GTPase Rab31 in cancer. J Cell Mol Med 19:1–10
11. Chua CE, Tang BL (2014) Engagement of the small GTPase Rab31 protein and its effector, early endosome antigen 1, is important for trafficking of the ligand-bound epidermal growth factor receptor from the early to the late endosome. J Biol Chem 289:12375–12389
12. Grismayer B, Solch S, Seubert B, Kirchner T, Schafer S, Baretton G, Schmitt M, Luther T, Kruger A, Kotzsch M, Magdolen V (2012) Rab31 expression levels modulate tumor-relevant characteristics of breast cancer cells. Mol Cancer 11:62
13. Jin C, Rajabi H, Pitroda S, Li A, Kharbanda A, Weichselbaum R, Kufe D (2012) Cooperative interaction between the MUC1-C oncoprotein and the Rab31 GTPase in estrogen receptor-positive breast cancer cells. PLoS One 7:e39432
14. Serao NV, Delfino KR, Southey BR, Beever JE, Rodriguez-Zas SL (2011) Cell cycle and aging, morphogenesis, and response to stimuli genes are individualized biomarkers of glioblastoma progression and survival. BMC Med Genom 4:49
15. Chan LH, Wang W, Yeung W, Deng Y, Yuan P, Mak KK (2014) Hedgehog signaling induces osteosarcoma development through Yap1 and H19 overexpression. Oncogene 33:4857–4866
16. Briscoe J, Therond PP (2013) The mechanisms of Hedgehog signalling and its roles in development and disease. Nat Rev Mol Cell Biol 14:416–429
17. Pan Y, Zhang Y, Chen L, Liu Y, Feng Y, Yan J (2016) The Critical Role of Rab31 in Cell Proliferation and Apoptosis in Cancer Progression. Mol Neurobiol 53:4431–4437
18. Cao CM, Yang FX, Wang PL, Yang QX, Sun XR (2014) Clinicopathologic significance of S100A4 expression in osteosarcoma. Eur Rev Med Pharmacol Sci 18:833–839
19. Enneking WF, Spanier SS, Goodman MA (2003) A system for the surgical staging of musculoskeletal sarcoma. 1980. Clin Orthop Relat Res 4–18. https://doi.org/10.1097/01.blo.0000093891.12372.0f
20. Vergara-Lluri ME, Moatamed NA, Hong E, Apple SK (2012) High concordance between HercepTest immunohistochemistry and ERBB2 fluorescence in situ hybridization before and after implementation of American Society of Clinical Oncology/College of American Pathology 2007 guidelines. Mod Pathol 25:1326–1332
21. Warzecha J, Gottig S, Chow KU, Bruning C, Percic D, Boehrer S, Brude E, Kurth A (2007) Inhibition of osteosarcoma cell proliferation by the Hedgehog-inhibitor cyclopamine. J Chemother 19:554–561
22. Li S, Sun W, Wang H, Zuo D, Hua Y, Cai Z (2015) Research progress on the multidrug resistance mechanisms of osteosarcoma chemotherapy and reversal. Tumour Biol 36:1329–1338
23. Yamamoto N, Tsuchiya H (2013) Chemotherapy for osteosarcoma—where does it come from? What is it? Where is it going? Expert Opin Pharmacother 14:2183–2193
24. Yang D, Liu G, Wang K (2015) miR-203 acts as a tumor suppressor gene in osteosarcoma by regulating RAB22A. PLoS One 10:e0132225
25. Shahi MH, Holt R, Rebhun RB (2014) Blocking signaling at the level of GLI regulates downstream gene expression and inhibits proliferation of canine osteosarcoma cells. PLoS One 9:e96593
26. Hirotsu M, Setoguchi T, Sasaki H, Matsunoshita Y, Gao H, Nagao H, Kunigou O, Komiya S (2010) Smoothened as a new therapeutic target for human osteosarcoma. Mol Cancer 9:5
27. Wang W, Luo H, Wang A (2006) Expression of survivin and correlation with PCNA in osteosarcoma. J Surg Oncol 93:578–584
28. Piro F, Leonardi L (2015) Expression of Bcl-2 in canine osteosarcoma. Open Vet J 5:27–29
29. Wang D, Bi Z (2014) Bufalin inhibited the growth of human osteosarcoma MG-63 cells via down-regulation of Bcl-2/Bax and triggering of the mitochondrial pathway. Tumour Biol 35:4885–4890
30. Wuichet K, Sogaard-Andersen L (2014) Evolution and diversity of the Ras superfamily of small GTPases in prokaryotes. Genome Biol Evol 7:57–70
31. Warzecha J, Dinges D, Kaszap B, Henrich D, Marzi I, Seebach C (2012) Effect of the Hedgehog-inhibitor cyclopamine on mice with osteosarcoma pulmonary metastases. Int J Mol Med 29:423–427
32. Paget C, Duret H, Ngiow SF, Kansara M, Thomas DM, Smyth MJ (2012) Studying the role of the immune system on the antitumor activity of a Hedgehog inhibitor against murine osteosarcoma. Oncoimmunology 1:1313–1322
33. Saitoh Y, Setoguchi T, Nagata M, Tsuru A, Nakamura S, Nagano S, Ishidou Y, Nagao-Kitamoto H, Yokouchi M, Maeda S, Tanimoto A, Furukawa T, Komiya S (2016) Combination of Hedgehog inhibitors and standard anticancer agents synergistically prevent osteosarcoma growth. Int J Oncol 48:235–242

34. Ding YL, Zhou Y, Xiang L, Ji ZP, Luo ZH (2012) Expression of glioma-associated oncogene homolog 1 is associated with invasion and postoperative liver metastasis in colon cancer. Int J Med Sci 9:334–338
35. Tao Y, Mao J, Zhang Q, Li L (2011) Overexpression of Hedgehog signaling molecules and its involvement in triple-negative breast cancer. Oncol Lett 2:995–1001
36. You S, Zhou J, Chen S, Zhou P, Lv J, Han X, Sun Y (2010) PTCH1, a receptor of Hedgehog signaling pathway, is correlated with metastatic potential of colorectal cancer. Ups J Med Sci 115:169–175
37. Sui Y, Zheng X, Zhao D (2015) Rab31 promoted hepatocellular carcinoma (HCC) progression via inhibition of cell apoptosis induced by PI3K/AKT/Bcl-2/BAX pathway. Tumour Biol 36:8661–8670
38. Lo WW, Wunder JS, Dickson BC, Campbell V, McGovern K, Alman BA, Andrulis IL (2014) Involvement and targeted intervention of dysregulated Hedgehog signaling in osteosarcoma. Cancer 120:537–547
39. Eggenschwiler JT, Espinoza E, Anderson KV (2001) Rab23 is an essential negative regulator of the mouse Sonic hedgehog signalling pathway. Nature 412:194–198